Journal of The Electrochemical Society, **160** (11) A2244-A2250 (2013)
0013-4651/2013/160(11)/A2244/7/$31.00 © The Electrochemical Society

Bi-Functional N-Doped CNT/Graphene Composite as Highly Active and Durable Electrocatalyst for Metal Air Battery Applications

Hey Woong Park,[a] Dong Un Lee,[a] Yulong Liu,[a,*] Jason Wu,[a] Linda F. Nazar,[b] and Zhongwei Chen[a,z]

[a]*Department of Chemical Engineering, Waterloo Institute for Nanotechnology, Waterloo Institute for Sustainable Energy, University of Waterloo Waterloo, Ontario N2L 3G1, Canada*
[b]*Department of Chemistry, Waterloo Institute for Nanotechnology, University of Waterloo, Waterloo, Ontario N2L 3G1, Canada*

Ethylene diamine-based nitrogen doped carbon nanotube (NCNT) was successfully synthesized on thermally reduced graphene oxide (TRGO) by an injection chemical vapor deposition method and its electrocatalytic activities for oxygen reduction and evolution reactions (ORR and OER, respectively) were investigated for metal air battery applications. The TRGO/NCNT composite with a novel bridged planes morphology does not only exhibits ORR performance similar to that of commercial Pt/C catalyst, but also demonstrates a superior OER activity. Furthermore, the composite exhibits an excellent electrochemical durability confirmed by full range cyclic voltammetry (CV) cycling. This study highlights an approach to prepare highly active and durable metal free catalysts as a highly efficient electrode material for rechargeable metal air battery applications.
 [DOI: 10.1149/2.097311jes]

Manuscript submitted August 8, 2013; revised manuscript received September 30, 2013. Published October 15, 2013.

Electrochemical energy conversion systems such as batteries, supercapacitors and fuel cells are continuously being pushed by intensive research efforts in order to meet the ever increasing demands for energy. Ultimately, newly developed energy devices aim to replace the conventional combustion systems that generate energy by burning natural resources such as fossil fuels since they have been recognized as main contributor to the greenhouse gases which have approached a critical level for the survival of human beings. It has been clearly understood that amongst many systems, Lithium (Li) ion batteries are considered as the most advanced and attractive since they offer rechargeability with a high efficiency, energy density and durability in substance, compared to other systems. However, metal air batteries especially attract energy research interest because they possess much higher theoretically energy density than the state-of-the-art Li ion battery, and they have the potential to be rechargeable in contrast to fuel cells.[1] Based on the reaction mechanisms in generating and storing electric energy in a metal air battery, redox reactions between a metal and oxygen are the main features. While the battery is in operation, the overall reaction kinetics relies on the rates of oxygen reduction reaction (ORR) and oxygen evolution reaction (OER) as the system produces and stores electric energy, respectively. However, the rates of these reactions are too sluggish to meet the requirements for practical applications.[1,2] Therefore, a highly active bi-functional catalyst that significantly enhances the kinetics of both oxygen reactions in a cathode is vital for realization of wide commercialization of the metal air battery technology.

To date, precious platinum (Pt) metal exhibits the best electrocatalysis during ORR with a swift reduction process of oxygen, so nano-sized Pt combined with carbon materials and Pt alloying are employed in the orthodox fuel cell technologies as a catalyst.[3–9] However, high costs and poor durability of the precious metal catalysts push the fuel cell and the metal air battery technologies to be more cost competitive and become viable energy systems for practical applications. Alternatively, promising approaches with non-precious transition metal oxides have been tremendously proposed introducing the reasonable performances.[10,11] Besides, OER has emerged as a critical area of improvement since the rechargeable metal air batteries have settled down on attractive energy storage systems.[12] Relatively expensive iridium (Ir) or ruthenium (Ru)-based materials have been reported as an excellent OER catalyst in alkaline media; however, its ORR activity is much lower than that of other transition metal oxides, which makes this catalyst unsuitable for rechargeable applications.[13,14] Therefore, developing efficient and affordable bi-functional catalysts is crucial for further advancement of rechargeable metal air battery technology.

Most of metal and metal oxide catalysts have been practically utilized in combination with a carbon black support to improve the electrical conductivity and reduce the amount of the catalyst loadings in an electrode. Amongst a variety of carbon support materials, graphene-based materials have been the center of attention since they possess unique two-dimensional morphologies with high surface area, reasonable chemical resistance and excellent electronic conductivity.[15] Metal and metal oxide decorated graphene materials have been introduced as electrochemical catalysts, presenting enhanced ORR performance and durability compared to conventional carbon black supports.[16–19] Furthermore, graphene itself demonstrates outstanding electrocatalytic activity, especially when they are doped with heteroatoms such as boron, nitrogen and sulfur, boasting its capabilities in various applications.[20–22] However, during the preparation of the electrode, graphene-based materials tend to restack due to strong Van der Waals interactions resulting in the loss of their catalytic activities.[15,23] In addition, there is a lack of OER studies on graphene materials based on our best knowledge; hence we investigate them in this study along with ORR activities for bi-functional capabilities.

Herein, we propose metal free thermally reduced graphene oxide (TRGO) based electrochemical catalyst for rechargeable metal air battery applications. Most of previous reports on graphene based catalysts have employed chemically reduced graphene oxide (RGO) because it can be prepared in large quantities and is convenient for combining with metal or metal oxide catalysts as composites.[17,24,25] However, the thermal annealing method is simple and environmental friendly as no additional use of chemical is required for the reduction process.[21] In addition, the thermal annealing technique leads to greater expansion of the graphene sheets and the formation of defects and edge sites in the graphitic network, which have been suggested as highly active catalytic sites for the oxygen reactions.[26,27] Despite of these merits of this simple thermal annealing process, this method leads to the loss of long range electrical conductivity since the planar sheets of aromatic carbon network are physically separated by high pressure gas generated during the reaction.[21] To compensate this, nitrogen doped-carbon nanotubes (NCNT) is utilized in this work to serve a critical role as a bridge to electrically connect the discrete graphene sheets, thereby restoring the electrical conductivity. Conversely, TRGO plays a role of the substrate to support electrical inter-connections between NCNTs. Moreover, we strongly believe that this addition of NCNT onto graphene sheet as a composite structure can prevent the sheets from restacking during electrode fabrication. In addition to the structural merits,

*Electrochemical Society Student Member.
zE-mail: zhwchen@uwaterloo.ca

it is worth noting that NCNT can obviously provide highly catalytic active sites through nitrogen doping. Recently, Li et al., have synthesized iron-containing nitrogen-doped graphene-carbon nanotube complexes as an ORR catalyst by unzipping the outer graphitic layers of the multi-walled CNT using a highly oxidizing reagent followed by an annealing process in NH_3 at an elevated temperature.[28] In contrast to the present study, they have reported that the nitrogen-doped graphene demonstrates highly catalytic activity with CNT allowing fast charge transport. Ma et al., have also introduced NCNT on chemically reduced graphene oxide with a three-dimensional structure as a metal free electrocatalyst.[24] However, its ORR performance was not only inferior to that of Pt/C but their investigation was also limited to oxygen reduction catalytic activity. Presumably, the limited performance is attributed to the pyridine-derived NCNT. According to the literature, the ORR performance of pyridine-derived NCNT cannot surpass that of ethylene diamine (EDA)-derived NCNT due to the higher nitrogen content and the nitrogen configuration of EDA-derived NCNT.[29] In this study, we employ EDA as a carbon source to prepare NCNT directly on TRGO which have shown an outstanding catalytic activity demonstrated in the previous work.[29] As a result, the electrochemical catalytic activity of ORR with TRGO/NCNT hybrid composite in this study reveals comparable performance to that of state-of-the-art ORR catalyst, Pt/C. Furthermore, this graphitic carbon hybrid material demonstrates an impressive OER activity with excellent durability, indicating the superior ORR activity to Pt/C after a full range cyclic voltammetry (CV) cycling test. The hybrid TRGO/NCNT composite based on our electrochemical investigation demonstrates feasibility as a bi-functional catalyst for rechargeable metal air batteries.

Experimental

A brief schematic diagram of the synthesis of TRGO/NCNT composite is illustrated in Scheme 1. One step thermally reduced graphene (TRGO) was synthesized as described in the previous report.[25] First, graphite oxide (GO) is prepared by a modified Hummer's method from natural graphite, and then GO is placed in a quartz tube outside of the heating area of the horizontal tube furnace. When the temperature of the furnace reaches to 1000°C under 100 sccm of Ar gas stream, the quartz tube is quickly shifted for GO to be placed in the heating area in the center of the furnace and kept in that position for 30 ∼ 60 seconds. This rapid thermal process have enabled GO to be reduced and exfoliated. The tube is taken back after the thermal treatment outside of the heating area of the furnace and TRGO is collected. To prepare TRGO/NCNT composite, injection chemical vapor deposition (CVD) method have been conducted to grow NCNT on TRGO. The prepared TRGO is mixed with 0.25 mL of 0.5 wt% ferrocene (C10H10Fe, Aldrich) dissolved ethanol solution. The mixture is casted inside of a small quartz tube (18 mm O.D., 100 mm length) and then the small tube is positioned in the heating zone of a horizontal tube furnace. As a precursor of the injection CVD method for NCNT, 1.0 mL of 2.5 wt% ferrocene containing ethylene diamine (C2H8N2, Aldrich) is loaded into a syringe for the injection. The precursor is injected at 0.05 mL min^{-1} to produce NCNT under the nitrogen flow at 100 sccm and 700°C. After the reaction, the black powder at the position of TRGO in the small tube is collected as TRGO/NCNT composite. The rest of the black powder is also collected as pure NCNT to compare with the composite. Lastly, TRGO/NCNT and NCNT is washed with 0.5 M H_2SO_4 solution to leach out the ferrocene derived materials out similar to our previous reports.[29]

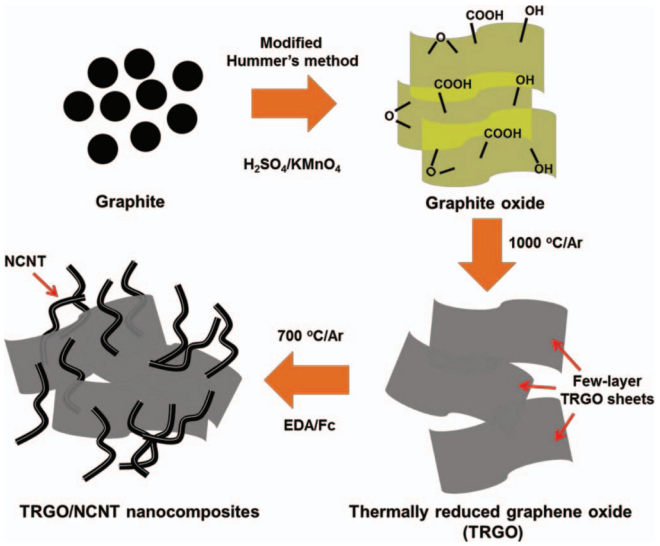

Scheme 1. Schematic diagram of the synthesis of TRGO/NCNT composite.

For the characterizations of the prepared materials, X-ray diffraction (XRD) was used to investigate the oxidation of natural graphite and reduction of GO, and growth of NCNT. Scanning electron microscopy (SEM) (LEO FESEM 1530) and transmission electron microscopy (TEM) (JEOL 2010F) were utilized to confirm the morphology and structure of TRGO and TRGO/NCNT composite. X-ray photoelectron spectroscopy (XPS) (Thermal Scientific K-Alpha XPS spectrometer) was conducted to detect the atomic composition of elements in the TRGO and TRGO/NCNT.

The electrocatalytic activity and durability of the catalyst samples were examined using rotating disk electrode (RDE) voltammetry by a potentiostat (CH Instrument 760D) and a rotation speed controller (Pine Instrument Co., AFMSRCE). The catalyst materials were dispersed in ethanol-diluted Nafion solution to be 4 mg mL^{-1} of the catalyst concentration and coated on glassy carbon disk electrodes (5 mm OD) with 20 μL of the ink (loading 0.41 mg cm^{-2})for the working electrode. A platinum (Pt) wire and saturated calomel electrode (SCE) were utilized as counter and reference electrodes, respectively. Cyclic voltammetry (CV) is used to investigate ORR and OER activities with durability in O_2 and N_2-saturated 0.1 M KOH at a scan rate of 50 mV s^{-1}. Linear sweep voltammetry (LSV) is used for further examination of ORR activity in RDE measurements at a scan rate of 10 mV s^{-1} in the same electrolyte.

Results and Discussion

Figure 1 shows the XRD patterns of TRGO and TRGO/NCNT with a broad diffraction peak for (002) plane in the range 22 ∼ 27° which are typical characteristics of few-layer reduced graphene oxide and CNT materials.[15,25,30] However, two patterns display different features. The pattern of TRGO suggests that even though GO was heat treated less than one minute at 1000°C, it was well reduced and exfoliated to graphene as observed by the broad peak and relatively low intensity of the peak. On the contrary, the hybrid TRGO/NCNT composite possesses relatively higher angle and intensity compared to TRGO. The pattern is attributed to the multi-walled nature of the NCNT.[30] The number and d-spacing of the graphene layers in NCNT is larger and shorter than those of TRGO, respectively, resulting in a sharper peak at a slightly higher angle. The inset of Figure 1a presents the XRD pattern with a relatively sharp peak at ∼11.5° of GO prepared from natural graphite by the modified Hummer's method to compare with the pattern of graphene-based materials. It supports TRGO reduction from GO as the right-shift in the diffraction angle indicates decrease in the d-spacing. The elemental composition of the hybrid TRGO/NCNT composite is examined by X-ray photoelectron spectroscopy (XPS) characterization. Figure 1b introduces the full spectrum of the samples in XPS. There are three major peaks which correspond to carbon (C) 1s, nitrogen (N) 1s and oxygen (O) 1s and the diminutive trace of iron (Fe) 2p from the ferrocene catalyst. The peak at the 284.1 eV represents C 1s with the sp2 configuration indicating a majority of carbon is in the conjugated graphitic lattice. The peak corresponding to N 1s at 397.1 eV reveals that nitrogen is successfully doped into the CNT matrix. The peak intensity of O 1s at 532.1 eV have increased

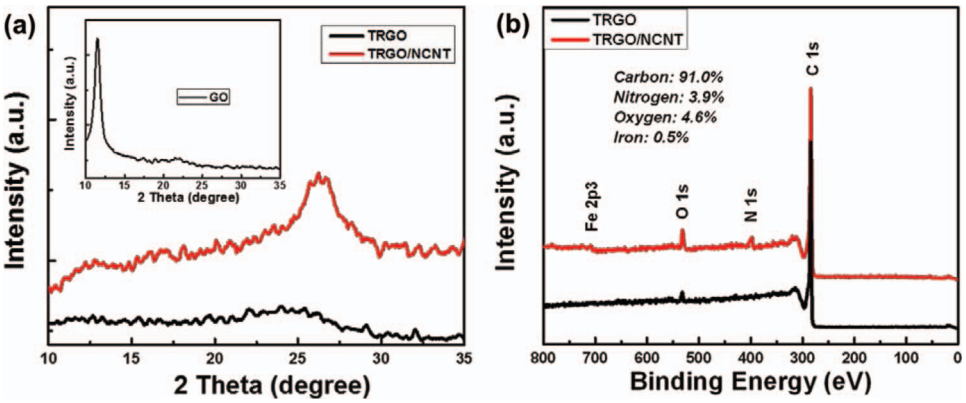

Figure 1. XRD patterns of (a) TRGO and TRGO/NCNT (inset: graphite oxide (GO)), and (b) full XPS spectra of TRGO and TRGO/NCNT.

during synthesis of NCNT, compared to that of TRGO due to the possible formation of pyridinic N^{+}-O^{-} during the synthesis[29] as well as adsorbed oxygen on carbon near the doped nitrogen species in the NCNT due to its affinity to oxygen.[25] In addition, the spectrum of NCNT/TRGO exhibits the total content ratio of the carbon, oxygen and nitrogen to be 91.0, 4.6, and 3.9%, respectively. It is expected that the nitrogen species in NCNT render the electrochemical catalytic active sites for ORR since doped nitrogen can produce defects sites related to high activity for oxygen.

Figure 2a and 2b demonstrate SEM images of the TRGO and TRGO/NCNT composite, respectively. The SEM image of TRGO shows a thin sheet morphology, indicative of the facile synthesis method by thermal treatment successfully reducing graphite oxide to graphene sheets.[31] As shown in Figure 2b, TRGO/NCNT composite has resulted in a good dispersion of NCNT on TRGO. NCNTs are observed to be present mostly on the graphene surface indicating that they are directly grown on the graphene. Moreover, Figure 2b shows NCNTs contact several graphene sheets so that it is expected to improve conductivity of the electrode. The TEM image of TRGO in Figure 2c clearly displays thin and wrinkled morphology of graphene as reported in other literatures.[31,32] The TEM image shown in Figure 2d supports the SEM analysis of TRGO/NCNT composite as NCNTs flourished on the graphene sheet, suggesting the porous structure can be formed between the graphene sheets. NCNTs seem to be stemming out of the graphene sheet (Figure 2d inset). It is noted that the black dots in the image are the residual iron-based materials from the ferrocene catalyst. Even though the composite have been washed with 0.5 M H_2SO_4, based on the procedure of a previous report,[29] the iron particulates still remained in the composite. It is possible that graphitic network have hindered these particles from leaching out, but the amount is negligible as detected by XPS and does not affect the catalytic activities.[24] The inset in the Figure 2d looks as NCNTs take root on the surface of TRGO. The TEM and SEM analysis have confirmed the expected morphology of the TRGO/NCNT composites in this study.

To investigate the surface area and pore size distributions (PSD), Brunauer-Emmett-Teller (BET) and Barrett–Joyner–Halenda (BJH) methods, respectively, have been carried out. Figure 3 exhibits nitrogen adsorption-desorption isotherms of TRGO and TRGO/NCNT composite at 77K, indicating that the hysteresis loops correspond to previous CNT and graphene works.[31,33] The surface areas of TRGO and TRGO/NCNT present 528.4 $m^2\ g^{-1}$ and 175.3 $m^2\ g^{-1}$, respectively. The large surface area of TRGO is another supporting evidence of successful thermal reduction of GO by the thermal annealing process. On the other hand, the composite of TRGO/NCNT shows smaller surface area than that of TRGO itself, which is likely attributed to NCNT because generally CNT yields smaller surface areas than that of graphene sheets.[31,33] However, the PSD of TRGO/NCNT is shifted to a larger size, compared to that of TRGO, as shown in Figure 3 inset. This is strong evidence that bolsters our earlier conjecture that the NCNT grown on the surface of graphene sheets help to prevent the sheets from restacking and providing spaces between graphene

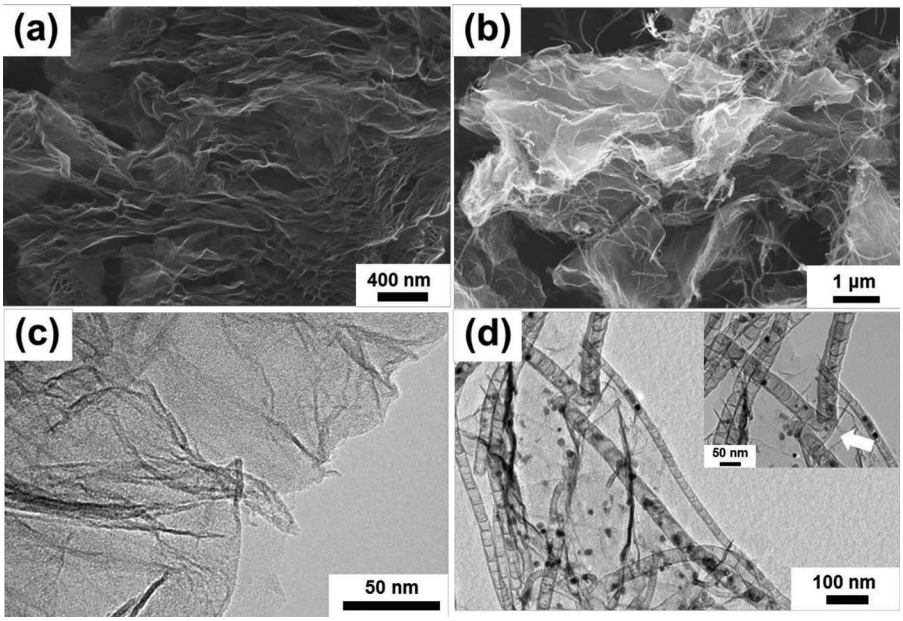

Figure 2. SEM images of (a) TRGO and (b) TRGO/NCNT, TEM images of (c) TRGO and (d) TRGO/NCNT (inset: magnified image).

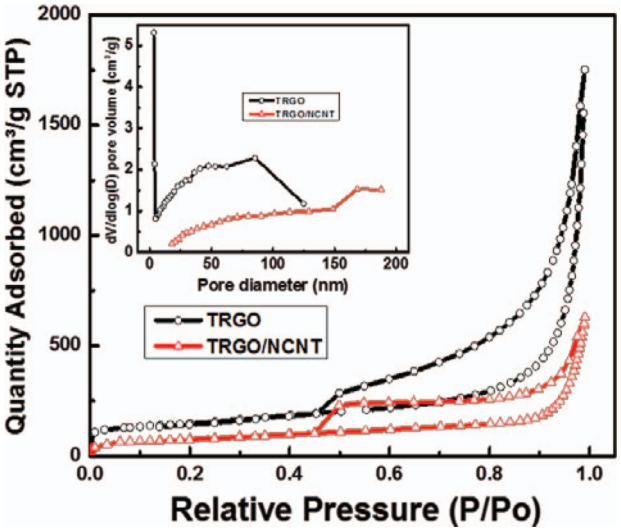

Figure 3. N_2 adsorption–desorption isotherms of TRGO and TRGO/NCNT (inset: pore size distribution).

sheets. It is believed that the suggested structure can enhance utilization of the electrolyte in an electrochemical cell through enlarged spaces between the sheets.

As shown in Figure 4a, the ORR capabilities of TRGO and TRGO/NCNT composites are examined by cyclic voltammetry (CV) in nitrogen (N_2) and oxygen (O_2) atmosphere. For both materials, there are no detectable peak currents observed in N_2 atmosphere; however, the significant current peaks have appeared in O_2 atmosphere, which indicate that the materials are catalytically ORR active. In addition, higher current density and more positive potential observed for the composite indicates that TRGO/NCNT is more catalytically active. For further electrochemical analysis of ORR catalytic activity, rotating disk electrode (RDE) voltammetry with various electrode rotating speeds have been conducted. Figure 4b presents ORR activities of TRGO/NCNT, TRGO and NCNT, which was prepared in the same reaction batch of TRGO/NCNT, via RDE measurements with a rotation speed of 900 rpm at a scan rate of 10 mV s^{-1}. All ORR current densities in this study are normalized by surface area of the disk electrode and background-corrected by current densities obtained in N_2-saturated 0.1M KOH solution. Although ORR capabilities of TRGO itself have been demonstrated, when TRGO is combined with NCNT, the activity is significantly enhanced in terms of all electrochemical indicators such as the onset potential, half-wave potential and limiting current density. The performance of the composite presents 123 mV

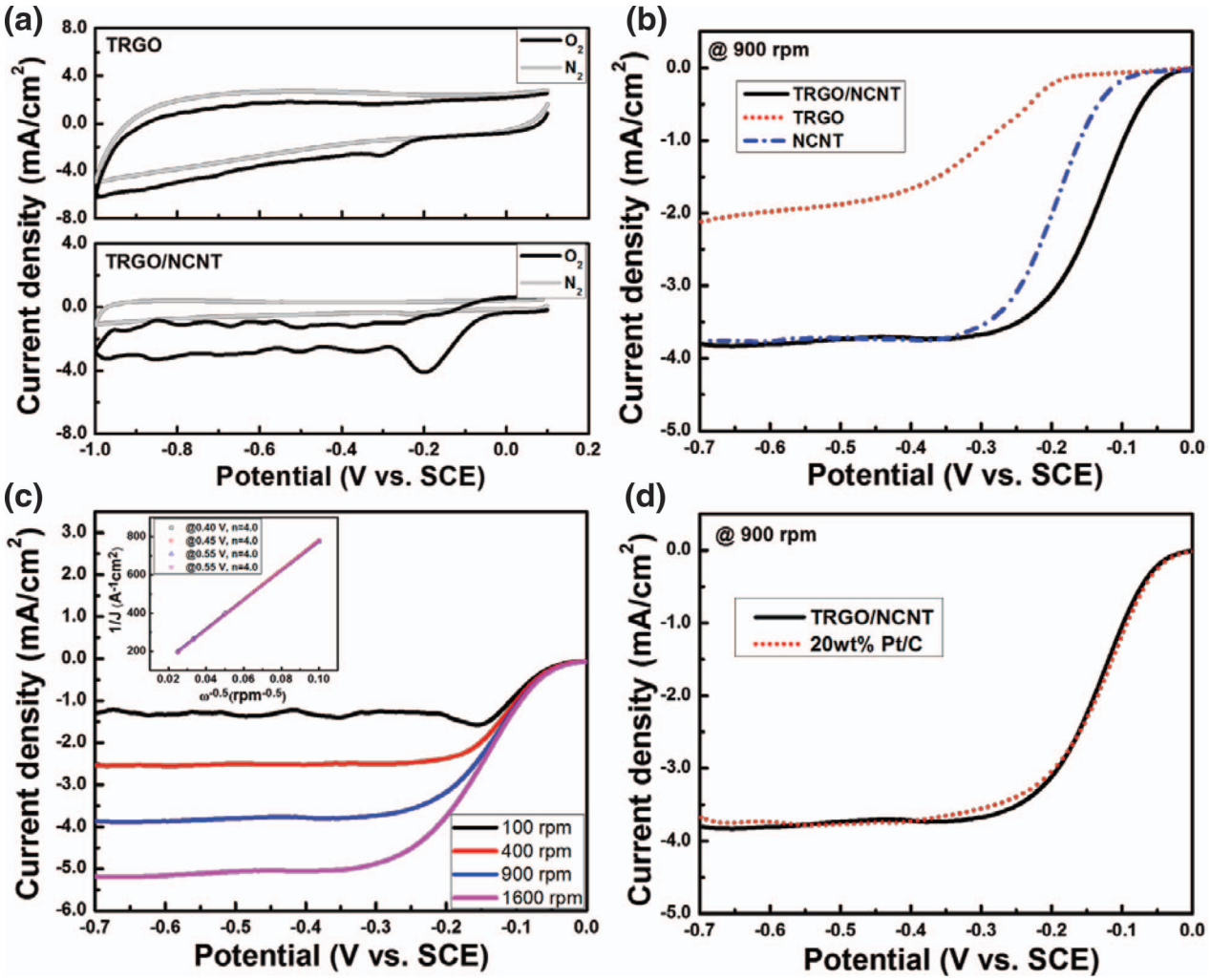

Figure 4. (a) Cyclic voltammograms of TRGO and TRGO/NCNT in N_2 and O_2 saturated 0.1M KOH, (b) ORR polarization curves of TRGO, NCNT and TRGO/NCNT at rotation speed of 900 rpm, (c) ORR polarization curves of TRGO/NCNT at various rotation speeds (inset: Koutecký-Levich plot at potentials −0.40, −0.45, −0.50 and −0.55 V (vs. SCE)) and (d) 20 wt% Pt/C with TRGO/NCNT at a rotation speed of 900 rpm.

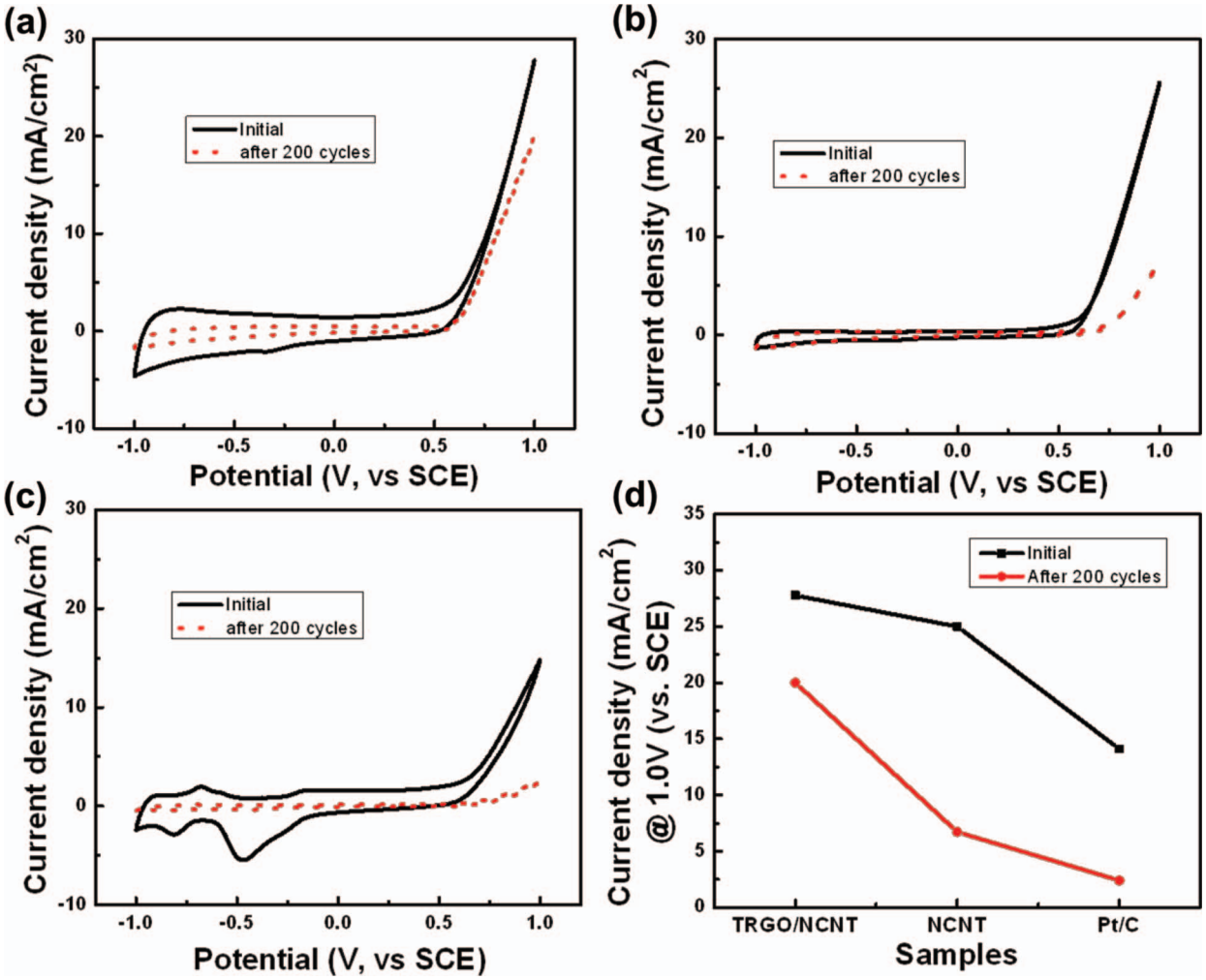

Figure 5. Cyclic voltammograms of (a) TRGO/NCNT, (b) NCNT, and (c) 20 wt% Pt/C for initial and after 200 cycles OER performances. (d) Comparison of the OER current density at 1.0 V (vs. SCE) of TRGO/NCNT, NCNT and 20 wt% Pt/C.

and 152 mV higher onset and half-wave potentials, respectively. In addition, it shows almost twice higher limiting current density at 0.5 V. It is believed that NCNT mainly contributes the improved activity since heteroatom doping in the graphitic layer is known to be the ORR catalytic active sites.[34–37] It also suggests that nitrogen species in the CNT can mainly engender the catalytic activity of the composite. Moreover, the TRGO/NCNT composite illustrates 48 mV and 60 mV improvements in terms of onset and half-wave potential, respectively, in comparison to those of NCNT. This is most probably due to the graphene sheets contributing in improving the activity facilitated by the nanotubes bridging the sheets to create electron pathways, generating useful pores, and preventing restacking of graphene sheets. Based on the RDE measurements of TRGO/NCNT at various rotation speeds as shown in Figure 4c, the degree of the ORR activity can be verified via the Koutechý-Levich (K-L) equation as the following,[10]

$$\frac{1}{i} = \frac{1}{i_k} + \frac{1}{i_d}$$

$$i_k = nFkC_o$$

$$i_d = 0.2nFD_O^{2/3}\upsilon^{-1/6}C_O\omega^{1/2}$$

In the above equation, i_k and i_d is the kinetic current and diffusion limiting current density, respectively. F is the Faraday constant (96 485 C mol^{-1}), k is the rate constant for ORR (m s^{-1}), D_o is the diffusion coefficient of O_2 (1.9×10^{-5} cm^2 s^{-1}) in 0.1 M KOH, υ is the kinematic viscosity of 0.1 M KOH (0.01 cm^2 s^{-1}), C_o is the concentration of O_2 in the electrolyte (1.1×10^{-6} mol cm^{-3}) and ω is the angular frequency of the rotation which correlate with rotation speed. By linear fitting the Koutecky-Levich plots of i^{-1} vs. $\omega^{-0.5}$, the electron number (n) involved in the ORR can be determined, as shown in Figure 4c inset. The number of electrons is calculated at four different potentials of −0.40, −0.45, −0.50 and −0.55 V to be n = 4.0. This is ascribed to the ORR occurring via a four-electron reduction pathway which is known to $O_2 + 2H_2O + 4e^- \rightarrow 4OH^-$, indicating a rapid ORR reaction kinetics. To further examine the ORR activity, the RDE measurement of TRGO/NCNT is compared to those of state-of-the-art commercial 20% Pt/C. As shown in Figure 4d, the TRGO/NCNT composite exhibits comparable ORR performance to that of a commercial 20% Pt/C catalyst suggesting the composites developed in this study possesses an excellent ORR catalytic activity. This result could also be highlighted in comparison with the performances from previous reports related to the Pt-based alloy catalysts in alkaline media.[38,39]

In addition to the ORR performance, oxygen evolution reaction (OER) capabilities and electrochemical durability of the composite have been tested to evaluate the rechargeability of metal air batteries. OER activity can be evaluated by the current density at 1.0 V (vs. SCE) as shown in Figure 5a-5c. Among the TRGO/NCNT, NCNT and Pt/C catalysts, the initial OER current density (27.8 mA cm^{-2} at 1.0 V) of TRGO/NCNT demonstrates outstanding OER activity with 6.5% and 85% higher current density, compared to NCNT and Pt/C,

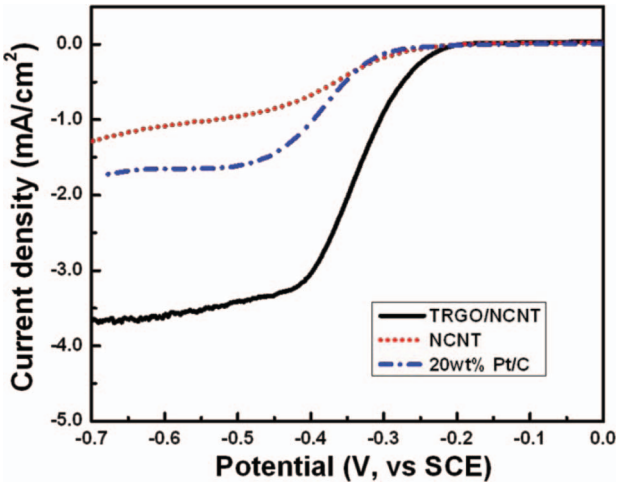

Figure 6. ORR polarization curves of TRGO/NCNT, NCNT and 20 wt% Pt/C at a rotation speed of 900 rpm after 200 full range CV cycles.

respectively. This value in combination with the ORR result indicates that the TRGO/NCNT is an excellent bi-functional OER and ORR catalyst, compare to other metal oxide-based catalysts.[10,40] In addition to ORR and OER activities, electrochemical durability of the catalysts in the operating voltage range is also a significant parameter especially in evaluating battery cycleability. To examine the durability of the catalysts, a full range CV between −1.0 V and 1.0 V (vs. SCE) in N_2-saturated 0.1M KOH solution have been conducted (Figure 5a-5c) and the summary of the initial and after 200 cycles OER current densities of TRGO/NCNT, NCNT and Pt/C catalysts is shown in Figure 5d. The difference of the current densities represents the durability of the catalysts so that the smallest change in current of TRGO/NCNT before and after cycle is a direct evidence of its excellent durability. Consequently, TRGO/NCNT presents 2.8 and 7.6 times higher OER current density than those of NCNT and Pt/C, respectively, after 200 CV cycles. According to the literatures, Pt/C can be degraded due to platinum agglomeration and dissolution, formation of platinum oxide, or separation from the carbon support during battery operation.[10] NCNT is known to be unstable for extended cycling, suffering from corrosion in the elevated potential.[41] However, the conductive network morphology created between the graphene sheets and NCNT most likely increases the rate of charge transfer in the electrode[28] and forms large porous structure which facilitates the electrolyte diffusion of hydroxide ion and oxygen.[42] These morphological features of the composite enhance the electrochemical kinetics for OER, ultimately mitigating highly undesirable side reactions such as carbon corrosion at high OER potentials. This leads to a highly durable electrode, which is observed in the long term OER cycling test of the composite. Lastly, RDE measurements at 900 rpm have been carried out to evaluate the retention of ORR activity after the full range CV cycling. As shown in Figure 6, Pt/C and NCNT catalysts present significant degradation of ORR performance attributed to the change of the catalytic surface, whereas the TRGO/NCNT composite outperforms the catalytic activity of Pt/C with twice higher limiting current density with 43 mV greater half-wave potential, confirming a long term catalytic effect of the proposed composite in this study for metal air battery applications.

Conclusion

In this study, the graphene was prepared by facile thermal annealing method from GO and then EDA-based NCNT directly bound to graphene composite by the CVD method has been introduced for the electrochemical catalysts for metal air batteries. The novel morphology of the NCNT-bridged TRGO composite was characterized by the SEM and TEM images and XPS results reveal chemical elements in TRGO/NCNT supporting nitrogen-doping of CNT during the injection CVD synthesis. The TRGO/NCNT in this study not only demonstrates comparable ORR activity to that of state-of-the-art Pt/C catalyst illustrating a four electron reduction pathway, but also highlights remarkable OER activity and excellent durability in the full voltage range. Furthermore, TRGO/NCNT outperforms Pt/C for ORR even after the full range CV test for the evaluation of durability. Consequently, this study proposes the combination of two promising graphitic carbons with novel morphologies by a simple synthetic route. Based on the results that are associated with the excellent electrocatalytic activities with stability, it is revealed that this approach can create promising catalysts for rechargeable metal air batteries.

Acknowledgment

This research was supported by the Natural Sciences and Engineering Research Council of Canada (NSERC) through grants to Dr. Zhongwei Chen, and the University of Waterloo.

References

1. J.-S. Lee, S. Tai Kim, R. Cao, N.-S. Choi, M. Liu, K. T. Lee, and J. Cho, *Advanced Energy Materials*, **1**, 34 (2011).
2. F. Cheng and J. Chen, *Chemical Society Reviews*, **41**, 2172 (2012).
3. J. K. Nørskov, J. Rossmeisl, A. Logadottir, L. Lindqvist, J. R. Kitchin, T. Bligaard, and H. Jónsson, *The Journal of Physical Chemistry B*, **108**, 17886 (2004).
4. S. S. Zhang, X. Z. Yuan, J. N. C. Hin, H. J. Wang, K. A. Friedrich, and M. Schulze, *Journal of Power Sources*, **194**, 588 (2009).
5. K. Lee, M. Kim, and H. Kim, *Journal of Materials Chemistry*, **20**, 3791 (2010).
6. B. Lim, M. Jiang, P. H. C. Camargo, E. C. Cho, J. Tao, X. Lu, Y. Zhu, and Y. Xia, *Science*, **324**, 1302 (2009).
7. V. R. Stamenkovic, B. Fowler, B. S. Mun, G. Wang, P. N. Ross, C. A. Lucas, and N. M. Marković, *Science*, **315**, 493 (2007).
8. R. I. Jafri, T. Arockiados, N. Rajalakshmi, and S. Ramaprabhu, *Journal of The Electrochemical Society*, **157**, B874 (2010).
9. B. Luo, S. Xu, X. Yan, and Q. Xue, *Journal of The Electrochemical Society*, **160**, F262 (2013).
10. Z. Chen, A. P. Yu, D. Higgins, H. Li, H. J. Wang, and Z. W. Chen, *Nano Letters*, **12**, 1946 (2012).
11. J.-S. Lee, G. S. Park, H. I. Lee, S. T. Kim, R. Cao, M. Liu, and J. Cho, *Nano Letters*, **11**, 5362 (2011).
12. J. Suntivich, K. J. May, H. A. Gasteiger, J. B. Goodenough, and Y. Shao-Horn, *Science*, **334**, 1383 (2011).
13. Y. Gorlin and T. F. Jaramillo, *Journal of the American Chemical Society*, **132**, 13612 (2010).
14. Y. Lee, J. Suntivich, K. J. May, E. E. Perry, and Y. Shao-Horn, *Journal of Physical Chemistry Letters*, **3**, 399 (2012).
15. A. Yu, H. W. Park, A. Davies, D. C. Higgins, Z. Chen, and X. Xiao, *The Journal of Physical Chemistry Letters*, **2**, 1855 (2011).
16. B. Seger and P. V. Kamat, *The Journal of Physical Chemistry C*, **113**, 7990 (2009).
17. Y. Liang, Y. Li, H. Wang, J. Zhou, J. Wang, T. Regier, and H. Dai, *Nat Mater*, **10**, 780 (2011).
18. M. H. Seo, S. M. Choi, H. J. Kim, and W. B. Kim, *Electrochemistry Communications*, **13**, 182 (2011).
19. D. U. Lee, B. J. Kim, and Z. Chen, *Journal of Materials Chemistry A*, **1**, 4754 (2013).
20. Z.-H. Sheng, H.-L. Gao, W.-J. Bao, F.-B. Wang, and X.-H. Xia, *Journal of Materials Chemistry*, **22**, 390 (2012).
21. H. Wang, T. Maiyalagan, and X. Wang, *Acs Catalysis*, **2**, 781 (2012).
22. Y. Li, J. Wang, X. Li, D. Geng, M. N. Banis, Y. Tang, D. Wang, R. Li, T.-K. Sham, and X. Sun, *Journal of Materials Chemistry*, **22**, 20170 (2012).
23. E. Yoo, J. Kim, E. Hosono, H.-s. Zhou, T. Kudo, and I. Honma, *Nano Letters*, **8**, 2277 (2008).
24. Y. Ma, L. Sun, W. Huang, L. Zhang, J. Zhao, Q. Fan, and W. Huang, *The Journal of Physical Chemistry C*, **115**, 24592 (2011).
25. H. W. Park, D. U. Lee, L. F. Nazar, and Z. Chen, *Journal of The Electrochemical Society*, **160**, A344 (2013).
26. S. F. Pei and H. M. Cheng, *Carbon*, **50**, 3210 (2012).
27. E. Yoo and H. S. Zhou, *Acs Nano*, **5**, 3020 (2011).
28. Y. G. Li, W. Zhou, H. L. Wang, L. M. Xie, Y. Y. Liang, F. Wei, J. C. Idrobo, S. J. Pennycook, and H. J. Dai, *Nature Nanotechnology*, **7**, 394 (2012).
29. Z. Chen, D. Higgins, H. Tao, R. S. Hsu, and Z. Chen, *The Journal of Physical Chemistry C*, **113**, 21008 (2009).
30. S. Y. Chew, S. H. Ng, J. Wang, P. Novak, F. Krumeich, S. L. Chou, J. Chen, and H. K. Liu, *Carbon*, **47**, 2976 (2009).
31. Y. L. Li, J. J. Wang, X. F. Li, D. S. Geng, R. Y. Li, and X. L. Sun, *Chemical Communications*, **47**, 9438 (2011).
32. J.-Y. Choi, D. Higgins, and Z. Chen, *Journal of The Electrochemical Society*, **159**, B86 (2011).

33. Y. L. Li, J. J. Wang, X. F. Li, J. Liu, D. S. Geng, J. L. Yang, R. Y. Li, and X. L. Sun, *Electrochemistry Communications*, **13**, 668 (2011).
34. Y. Q. Sun, C. Li, and G. Q. Shi, *Journal of Materials Chemistry*, **22**, 12810 (2012).
35. Z. H. Sheng, H. L. Gao, W. J. Bao, F. B. Wang, and X. H. Xia, *Journal of Materials Chemistry*, **22**, 390 (2012).
36. Z. Yang, Z. Yao, G. Li, G. Fang, H. Nie, Z. Liu, X. Zhou, X. a. Chen, and S. Huang, *Acs Nano*, **6**, 205 (2011).
37. J. Liang, Y. Jiao, M. Jaroniec, and S. Z. Qiao, *Angewandte Chemie International Edition*, **51**, 11496 (2012).
38. H. T. Duong, M. A. Rigsby, W. P. Zhou, and A. Wieckowski, *Journal of Physical Chemistry C*, **111**, 13460 (2007).
39. F. H. B. Lima, C. D. Sanches, and E. A. Ticianelli, *Journal of The Electrochemical Society*, **152**, A1466 (2005).
40. F. Y. Cheng, J. A. Shen, B. Peng, Y. D. Pan, Z. L. Tao, and J. Chen, *Nature Chemistry*, **3**, 79 (2011).
41. Z. Chen, A. P. Yu, R. Ahmed, H. J. Wang, H. Li, and Z. W. Chen, *Electrochimica Acta*, **69**, 295 (2012).
42. K. P. Gong, F. Du, Z. H. Xia, M. Durstock, and L. M. Dai, *Science*, **323**, 760 (2009).